

# Geophysical Research Letters®










## RESEARCH LETTER

10.1029/2024GL109359

## Different Dynamics Drive Indian Ocean Moisture to the Southern Slope of Central Himalayas: An Isotopic Approach

### Key Points:

- Abnormally low  $\delta^{18}\text{O}_p$  values during the pre-monsoon season coincide with heavy precipitation events
- Occurrences of anomalous circulations lead to the abnormally low  $\delta^{18}\text{O}_p$  values during the pre-monsoon season
- Combined effects of the Indian summer monsoon and convection cause lower  $\delta^{18}\text{O}_p$  values during the monsoon season

Rong Guo<sup>1,2</sup>, Wusheng Yu<sup>1</sup> , Jingyi Zhang<sup>1</sup> , Stephen Lewis<sup>3</sup> , Lazhu<sup>4</sup>, Yaoming Ma<sup>1,2,5</sup> , Baiqing Xu<sup>1</sup> , Guangjian Wu<sup>1</sup> , Zhaowei Jing<sup>6</sup> , Pengjie Ren<sup>1,2</sup>, Zhuaxia Zhang<sup>1,2</sup>, Qiaoyi Wang<sup>1,2</sup>, and Dongmei Qu<sup>1</sup>

<sup>1</sup>State Key Laboratory of Tibetan Plateau Earth System, Environment and Resources (TPESER), Institute of Tibetan Plateau Research, Chinese Academy of Sciences, Beijing, China, <sup>2</sup>University of Chinese Academy of Sciences, Beijing, China, <sup>3</sup>Catchment to Reef Research Group, Centre for Tropical Water and Aquatic Ecosystem Research, James Cook University, Townsville, QLD, Australia, <sup>4</sup>Research Center for Ecology, School of Ecology and Environment, Tibet University, Lhasa, China, <sup>5</sup>College of Atmospheric Science, Lanzhou University, Lanzhou, China, <sup>6</sup>Laoshan Laboratory, Qingdao, China

### Supporting Information:

Supporting Information may be found in the online version of this article.

### Correspondence to:

W. Yu and J. Zhang,  
yuws@itpcas.ac.cn;  
zhangjingyi@itpcas.ac.cn

### Citation:

Guo, R., Yu, W., Zhang, J., Lewis, S., Lazhu, Ma, Y., et al. (2024). Different dynamics drive Indian Ocean moisture to the southern slope of central Himalayas: An isotopic approach. *Geophysical Research Letters*, 51, e2024GL109359. <https://doi.org/10.1029/2024GL109359>

Received 21 MAR 2024

Accepted 20 MAY 2024

**Abstract** This study uses precipitation oxygen isotopes ( $\delta^{18}\text{O}_p$ ) to examine key dynamics that deliver moisture to the southern slope of central Himalayas over different seasons. Results show that the majority of pre-monsoon  $\delta^{18}\text{O}_p$  values are relatively high and controlled by the westerlies and local moisture. However, some abnormally low  $\delta^{18}\text{O}_p$  values coincide with higher precipitation amounts during the pre-monsoon season due to moisture driven northwards from the Bay of Bengal and Arabian Sea to central Himalayas by anomalous circulations (quasi-anticyclone, anticyclone, or/and westerlies trough). The size and location of the quasi-anticyclone also influences the magnitude of the  $\delta^{18}\text{O}_p$  decrease. In comparison, the monsoon  $\delta^{18}\text{O}_p$  values are lower due to the combined effects of the Indian summer monsoon and convection. Our findings indicate that researchers need to consider the signals of abnormally low  $\delta^{18}\text{O}_p$  values during the pre-monsoon season when attempting to interpret ice core and tree-ring records from central Himalayas.

**Plain Language Summary** How moisture is transported to the southern slope of central Himalayas remains unclear, especially for the frequent heavy precipitation events that occur during the pre-monsoon season. Here, we address this issue using  $\delta^{18}\text{O}_p$  measurements from the Asang station on the southern slope of central Himalayas during 2018–2019. We find that some abnormally low  $\delta^{18}\text{O}_p$  values coincide with heavy precipitation during the pre-monsoon season. These abnormally low  $\delta^{18}\text{O}_p$  values are caused by the development of anomalous circulations that drives the Indian Ocean moisture to the Asang station. During the monsoon season, the  $\delta^{18}\text{O}_p$  values are much lower than other seasons. Such low values are the product of the combined effects of the Indian summer monsoon and convection. We propose that the abnormally low  $\delta^{18}\text{O}_p$  values during the pre-monsoon season need to be considered in paleoclimate reconstructions using ice core and tree-ring records in the region. The abnormally low  $\delta^{18}\text{O}_p$  values during the pre-monsoon season are closely correlated to anomalous circulations. This finding implies that  $\delta^{18}\text{O}_p$  records from ice core and tree ring archives may have potential to reconstruct the frequency and intensity of such anomalous circulations during the pre-monsoon season.

## 1. Introduction

The Himalayas are an important region of glaciation and provide the headwaters for many rivers (Bolch et al., 2012; Immerzeel et al., 2010; Scherler et al., 2011; Su et al., 2022; G. Zhang et al., 2023). As such, they provide a critical water resource for local and downstream areas (Acharya et al., 2020; Biemans et al., 2019; Shrestha & Aryal, 2011). In particular, central Himalayas have a number of meridional canyons that cut its southern slope and form important moisture transport channels (Bookhagen & Burbank, 2006, 2010; Hren et al., 2009). As a result, abundant moisture can be transported from the Indian Ocean and travel across central Himalayas onto the Tibetan Plateau. More importantly, numerous glaciers and dense forests also make the region a hot spot for paleoclimatic reconstructions using ice cores (Hou et al., 2019; Kang et al., 2002; Pang et al., 2014; Thompson et al., 2000; Yao et al., 1997) and tree rings (Brunello et al., 2019; Sano et al., 2013; Singh et al., 2021, 2022). The accurate interpretation of signals in these paleoclimatic archives is closely related to the understanding of moisture sources and moisture transport processes. Therefore, it is critical to study moisture sources and

© 2024. The Authors. Geophysical Research Letters published by Wiley Periodicals LLC on behalf of American Geophysical Union.

This is an open access article under the terms of the [Creative Commons Attribution License](https://creativecommons.org/licenses/by/4.0/), which permits use, distribution and reproduction in any medium, provided the original work is properly cited.

moisture transport over central Himalayas not only for understanding the water cycle but also to ensure accurate interpretation of paleoclimatic reconstructions.

Previous studies utilized meteorological data to suggest that the moisture for the southern Tibetan Plateau (including central Himalayas) is mainly derived from the Indian Ocean and the Bay of Bengal (Feng & Zhou, 2012; Pan et al., 2019). However, Curio et al. (2015) argued that less oceanic moisture can travel across the mountains (including central Himalayas) into the plateau, while the moisture on the plateau is mainly sourced to local moisture recycling (the recycling rate can reach as high as 63.2%). The causes for this contradictory conclusion are likely due to the different reanalysis data and the relatively low data resolution. In particular, due to the roughest and most complex terrain (including Mt. Everest and a number of meridional canyons), central Himalayas have sparse meteorological observation stations. In comparison, stable hydrogen and oxygen isotopes can fingerprint water sources as they are sensitive to environmental changes and can record water cycle information and trace moisture transport (Bowen & Wilkinson, 2002; Jing et al., 2022; Konecky et al., 2019; Yao et al., 2013; Yu et al., 2021; J. Zhang et al., 2021). Therefore, precipitation stable isotope data can make up for the deficiencies of scarce meteorological data and low resolution of reanalysis and satellite data, and provide a suitable approach to trace moisture sources and moisture transport over central Himalayas.

Indeed, previous studies have used oxygen isotope measurements in precipitation ( $\delta^{18}\text{O}_p$ ) in the Himalayas and adjacent regions to reveal moisture sources and moisture transport processes (Acharya et al., 2020; Adhikari et al., 2020; Axelsson et al., 2023; Chakraborty et al., 2016, 2022; Gao et al., 2011; Islam et al., 2021; Jeelani & Deshpande, 2017; Jeelani et al., 2018; Rahul & Ghosh, 2019; Ren et al., 2017; Sinha et al., 2019; Yu et al., 2016). For example, some studies have found that the  $\delta^{18}\text{O}_p$  values on the southern slope of the Himalayas change significantly in response to different moisture transported by the westerlies and the Indian summer monsoon (Acharya et al., 2020). Studies have shown that  $\delta^{18}\text{O}_p$  values are different from west to east along the southern foothills of the Himalayas, which indicates that the influences of the moisture transported from the Mediterranean Sea or Caspian Sea by the westerlies and moisture transported from the Indian Ocean by the Indian summer monsoon are different from west to east (Jeelani & Deshpande, 2017; Jeelani et al., 2018). However, comparatively less work has been done to determine moisture sources and moisture transport processes in central Himalayas using  $\delta^{18}\text{O}_p$  data. Hence, how the moisture from different sources is transported to central Himalayas by the westerlies and Indian summer monsoon remains unclear.

Unlike other parts of the Tibetan Plateau, the southern slope of central Himalayas often experiences heavy snowfall or rainfall during winter and spring in the pre-monsoon season (Lang & Barros, 2004; Sharma & Ganju, 2000; Wang et al., 2015). Such heavy snowfall or rainfall has a significant impact on glacier changes, plant growth and the production and life of herdsmen in the region (Acharya et al., 2020; Shrestha & Aryal, 2011). Therefore, it is of great significance to study the causes of such frequent snowstorms or rainstorms during the winter and spring seasons. However, the moisture sources and transport processes that drive these extreme events on the southern slope of central Himalayas is a major research gap.

This study aims to use stable isotopes in precipitation to examine how different transport dynamics drive the moisture from different sources to the southern slope of central Himalayas over different seasons, especially the moisture that drives the extreme events during the pre-monsoon season. To achieve this, we observed the daily  $\delta^{18}\text{O}_p$  values at the Asang station located on the southern slope of central Himalayas. First, we analyze the seasonal variations of  $\delta^{18}\text{O}_p$  at the sampling station. Second, we survey the moisture transport processes that affect the  $\delta^{18}\text{O}_p$  and focus on the anomalous circulations that appear to drive the extreme events during the pre-monsoon season. Finally, we document the influence of the Indian summer monsoon combined with convection on the  $\delta^{18}\text{O}_p$  during the monsoon season.

## 2. Materials and Methods

### 2.1. Study Sites and Stable Isotope Data

Asang station (27.41°N, 88.95°E, 2,800 m a.s.l.) is located in the Yadong Canyon on the southern slope of central Himalayas (Figure 1a and Figure S1 in Supporting Information S1). The daily  $\delta^{18}\text{O}_p$  observations from our sampling station (Figure 1a and Figure S1 in Supporting Information S1) covered the period 15 March 2018–6 October 2019 (Yu & Lazhu, 2023). The daily  $\delta^{18}\text{O}_p$  observations from the three sites of Tezpur, Darjeeling, and

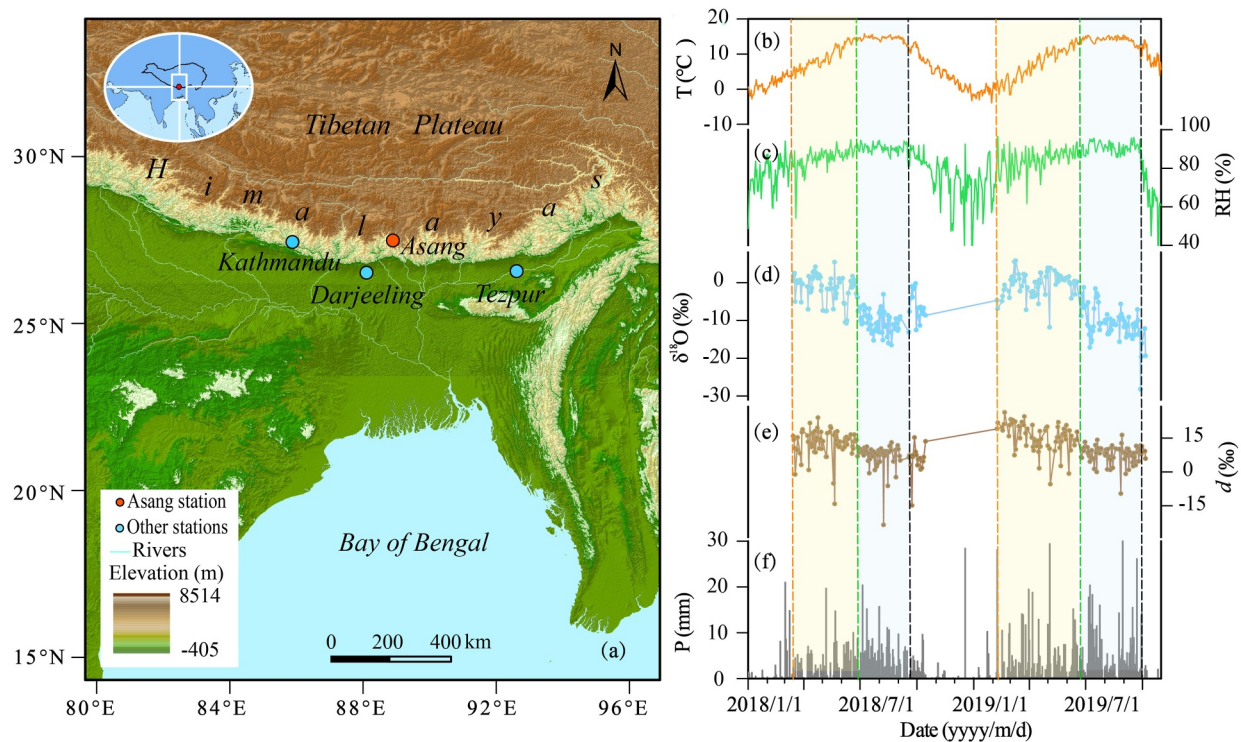


**Figure 1.** Location of the Asang station (red dot) and other stations (blue dots) including Tezpur, Darjeeling, and Kathmandu (a), and time series of air temperature ( $T$ ) (b), relative humidity (c),  $\delta^{18}\text{O}$  (d),  $d$ -excess ( $d$ ) (e), precipitation amount ( $P$ ) (f). The green and gray vertical dashed lines represent the dates of the Indian monsoon onset and retreat, respectively. The orange vertical dashed lines represent the starting date of the sampling. The pale yellow and light blue backgrounds represent the pre-monsoon season and monsoon seasons, respectively.

Kathmandu neighboring our station were obtained from Chakraborty et al. (2022) and Gao (2020), respectively (Text S1 in Supporting Information S1 for details).

## 2.2. Meteorological Data

To identify the circulation patterns and calculate the total water content, we used the reanalysis data derived from ERA5 ( $0.25 \times 0.25$ ) provided by the European Center for Medium-Range Weather Forecasts (ECWMF) (Hersbach et al., 2023a) (Text S2 in Supporting Information S1 for details).

## 3. Results

Daily  $\delta^{18}\text{O}_p$  values,  $d$ -excess values (Figures 1d and 1e) and corresponding air temperature, relative humidity (RH) and precipitation amounts (Figures 1b, 1c, and 1f) at the Asang station are shown in Figure 1. The daily  $\delta^{18}\text{O}_p$  values over the sampling period ranged from  $-28.25\text{‰}$  to  $5.79\text{‰}$ , with a mean of  $-5.84\text{‰} \pm 5.95\text{‰}$ . The corresponding  $d$ -excess values ranged from  $-23.54\text{‰}$  to  $26.37\text{‰}$ , with a mean of  $10.35\text{‰} \pm 6.55\text{‰}$ .

The  $\delta^{18}\text{O}_p$  values from 15 March to 27 June 2018 were relatively high (the mean value is  $0.70\text{‰} \pm 3.63\text{‰}$ ), but 19 abnormally low values (the mean value is  $-5.65\text{‰} \pm 2.69\text{‰}$ ) occurred during this period (Figure 1d). Over this period, the corresponding air temperatures gradually increased (Figure 1b), the precipitation amounts fluctuated and the relative humidities were generally high (Figures 1c and 1f). In comparison, the  $\delta^{18}\text{O}_p$  values from June 28 to 18 September 2018 exhibited a clear decreasing trend while the corresponding air temperatures, relative humidities and precipitation amounts were elevated. After 19 September 2018, the  $\delta^{18}\text{O}_p$  values gradually increased, while the air temperature, RH and precipitation amount decreased considerably and were opposite to the  $\delta^{18}\text{O}_p$  changes. Clearly, the  $\delta^{18}\text{O}_p$  values at Asang station showed considerable variability across the different seasons. Therefore, based on the pattern of the  $\delta^{18}\text{O}_p$ , the 2018 observation period can be divided into the pre-monsoon (15 March to 27 June 2018), monsoon (28 June to 18 September 2018), and post-monsoon (19 September to 15 October 2018) seasons. The dates of the Indian summer monsoon onset and retreat (Fasullo &

Webster, 2003) were on 28 June and 19 September 2018, respectively based on the corresponding sudden decrease and rapid increase of the  $\delta^{18}\text{O}_p$  (Figure 1d). The seasonal patterns of  $\delta^{18}\text{O}_p$  in 2019 were similar to those from 2018, so the observation period of 2019 was similarly divided (8 February to 17 June 2019, 24 June to 30 September 2019, and 5 October to 6 October 2019 as the pre-monsoon, monsoon, and post-monsoon seasons, respectively). The dates of the Indian monsoon onset and retreat were on 24 June and 5 October 2019, respectively based on the sudden decrease and rapid increase of the  $\delta^{18}\text{O}_p$  values. The monsoon onset and retreat dates are consistent with those from the north Indian region supported by Indian Meteorological Department (the onset dates in 2018 and 2019 were 24–26 June and 21–22 June, respectively; the retreat dates in 2018 and 2019 were 1–4 October and 12–13 October, respectively) (<https://reliefweb.int/report/india/india-meteorological-department-end-season-report-2018-southwest-monsoon> and <https://reliefweb.int/report/india/india-meteorological-department-end-season-report-2019-southwest-monsoon>). As our study site is located in the north of the north Indian region, the onset dates observed for our study site were later than those for the north Indian region and the retreat dates were earlier (Yu et al., 2016). During the pre-monsoon season, the majority of  $\delta^{18}\text{O}_p$  values were relatively high in both 2018 ( $-1.76\text{‰}$ – $5.40\text{‰}$ , accounts for 70% of pre-monsoon precipitation events) and 2019 ( $-1.90\text{‰}$ – $5.80\text{‰}$ , accounts for 72% of pre-monsoon precipitation events) (Figure 1d). We define these relatively high values as the “normal state” (Figures 1d and 3a, Figures S2a, S3a, S4a, and S8a in Supporting Information S1). However, some abnormally low  $\delta^{18}\text{O}_p$  values ( $<-2.00\text{‰}$ ) occurred during the pre-monsoon period (as low as  $-10.78\text{‰}$  and  $-11.84\text{‰}$  in 2018 and in 2019, respectively) and have been defined as the “abnormal cases” (Figures 1d, 3a, and 3b, Figures S2a, S3a, S4a, S8a, and S8b in Supporting Information S1). In addition, the seasonal variations of the  $\delta^{18}\text{O}_p$  values from Tezpur (Figure S2a in Supporting Information S1), Darjeeling (Figure S3a in Supporting Information S1), and Kathmandu (Figure S4a in Supporting Information S1) were similar to the observations from Asang. During the monsoon season, however, the majority of  $\delta^{18}\text{O}_p$  values (the mean value was  $-10.21\text{‰}$ ) are lower than the other seasons (Figure 1d). Moreover, those lower  $\delta^{18}\text{O}_p$  values persist from June to September, and the duration of these values is longer than other seasons (Figure 1d).

## 4. Discussion

### 4.1. $\delta^{18}\text{O}_p$ and Anomalous Circulations During the Pre-Monsoon Season

To investigate what caused the changes of  $\delta^{18}\text{O}_p$  values between the normal state and abnormal cases during the pre-monsoon season, we examined the horizontal moisture flux and wind fields (at 750, 600, and 500 hPa), as well as the winds at vertical levels and total water content fields in 2018 and 2019 (Figures 2 and 3, Figures S2–S4, S6, and S8 in Supporting Information S1).

For the normal state, we discuss the main reasons that lead to the relatively high  $\delta^{18}\text{O}_p$  values from both remote and local moisture sources. For the remote moisture sources, the Mediterranean region and the Atlantic Ocean act as the main source of precipitation for central Himalayas (Madhura et al., 2015; Tian et al., 2005), where the water vapor which is characterized by relatively high  $\delta^{18}\text{O}$  values is transported to our study area. Such relatively high water vapor  $\delta^{18}\text{O}$  values determine the high background values of the  $\delta^{18}\text{O}_p$  at the Asang station. Many studies likewise suggest this moisture source (Mediterranean Sea) is the main reason for the high  $\delta^{18}\text{O}_p$  values on the southern slope of the Himalayas (Hussain et al., 2015; Tian et al., 2005). In addition, the moisture flux and wind fields indicate that the moisture is transported advectively by the westerlies (Figures 2a–2c) without an obvious uplift effect in the zonal vertical direction (Figures 3d and 4a, and Figure S8d in Supporting Information S1). This limited uplift is due to the relatively weaker convection (Figure 3c) Note that the outgoing longwave radiation (OLR) values are relatively high compared with those in the abnormal cases and monsoon season. Therefore, the rainout effect is relatively weak in the zonal vertical direction and the  $\delta^{18}\text{O}_p$  values are only slightly depleted. Due to the limited moisture transported from south to north, the uplift effect in the meridional vertical direction on the  $\delta^{18}\text{O}_p$  is insignificant (Figure 3e and Figure S8e in Supporting Information S1).

For the local moisture source, Figures 2b and 2c show that moisture flux is relatively high near the site during the normal state. Therefore, relatively strong recirculating moisture from ecosystem productivity may also play an important role in producing the relatively high  $\delta^{18}\text{O}_p$  values (Figure 3a). Such local contributions were also confirmed by Chakraborty et al. (2022) and Adhikari et al. (2020) at the stations of Tezpur, Darjeeling, and Kathmandu that neighbor our study site. It is clear that both the remote and local moisture sources lead to the relatively high  $\delta^{18}\text{O}_p$  values at the Asang station for the normal state during the pre-monsoon season. The corresponding high d-excess values for the normal state imply that the mixing of dry air from relatively low-humidity

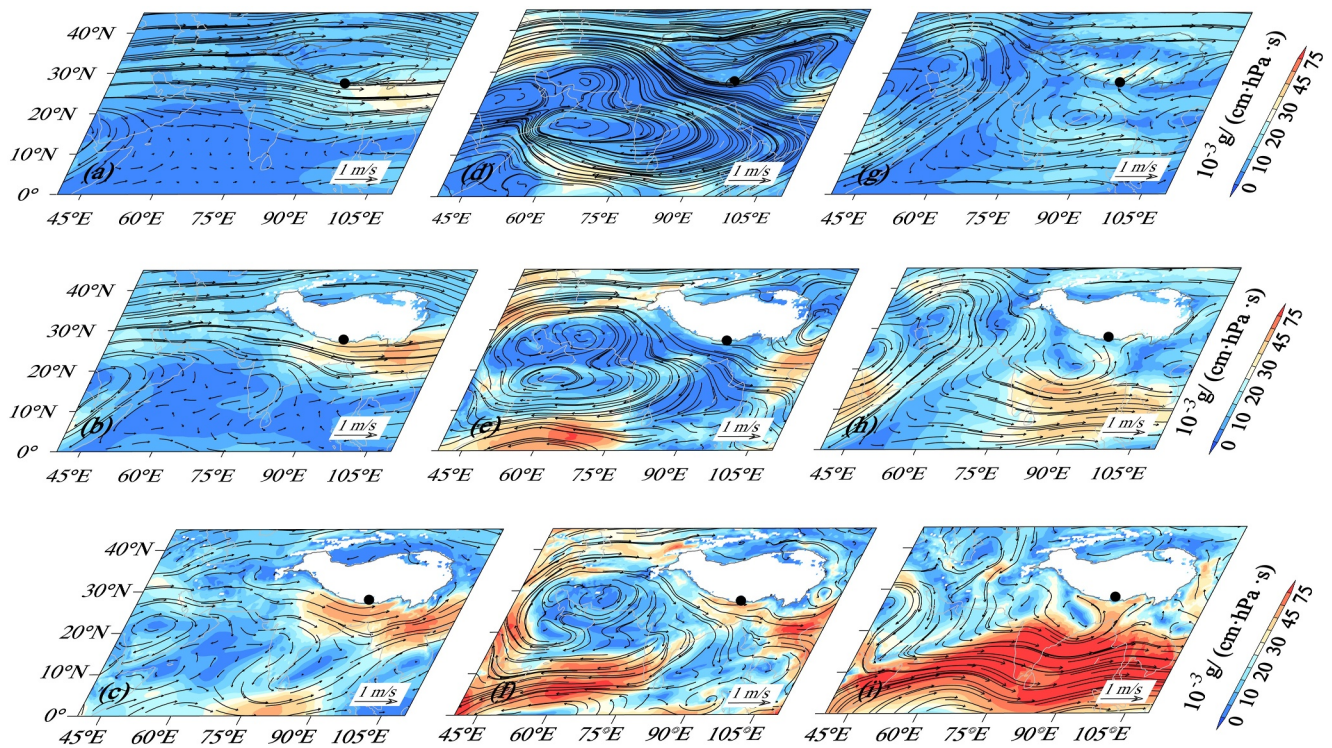


**Figure 2.** Moisture flux and wind fields over the Asang station at 750 hPa (c, f, i), 600 hPa (b, e, h), and 500 hPa (a, d, g) during the pre-monsoon (the normal state and abnormal cases) and monsoon seasons in 2018. Panels (a–c) represent the normal state during the pre-monsoon season. Panels (d–f) represent the abnormal cases during the pre-monsoon season (28 March 2018 was selected as an example, and other two examples of 8 April and 7 May in 2018 are shown in Figures S5 in Supporting Information S1). Panels (g–i) represent the monsoon season. The shading represents the water vapor flux, the arrows represent the wind field, and the black dot represents the Asang station. The white shadow represents areas above 3,500 m (c, f, i) and 4,000 m (b, e, h) altitude on the Tibetan Plateau that have missing values.

regions through the westerlies and local recirculating moisture may occur over our study site. The similar patterns of the relatively high  $\delta^{18}\text{O}_p$  values measured at the nearby stations (Tezpur, Darjeeling, and Kathmandu) for the normal state during the pre-monsoon season and the corresponding moisture flux and wind fields further support our conclusion (Figures S2b–S2d, S3b–S3d, and S4b–S4d in Supporting Information S1).

It should be pointed out that a trough of the subtropical westerlies (defined as westerlies trough) develops at the south of the Indian subcontinent ( $0^\circ\text{N}$ – $8^\circ\text{N}$  and  $65^\circ\text{E}$ – $85^\circ\text{E}$ ) during the pre-monsoon season (Figure 2c and Figure S6c in Supporting Information S1), as shown in Figure 4a. Indeed, at the front of the westerlies trough, abundant ocean moisture can be delivered to the east of the Himalayas, and even to the Hengduan Mountains (Yu et al., 2017) via the eastern Bay of Bengal. As a result, the  $\delta^{18}\text{O}_p$  values on the Hengduan Mountains are relatively low (Yu et al., 2017). However, our study site lies behind the westerlies trough. Hence, the westerlies trough operating during the normal state cannot contribute to the  $\delta^{18}\text{O}_p$  changes at the Asang station on the southern slope of central Himalayas.

For the abnormal cases, we use the  $\delta^{18}\text{O}_p$  values on 28 March, 8 April, and 7 May in 2018 (26 March, 6 April, and 9 April in 2019) as examples. Their  $\delta^{18}\text{O}_p$  values were as low as  $-5.21\text{‰}$ ,  $-7.06\text{‰}$ , and  $-7.55\text{‰}$  ( $-7.21\text{‰}$ ,  $-2.32\text{‰}$ , and  $-3.70\text{‰}$  in 2019), respectively (Figure 1d) and corresponded to precipitation amounts of 4.3, 7.0, and 19.7 mm (11.7, 18.8, and 3.2 mm in 2019), respectively (Figure 1f).

In the horizontal direction, unlike the normal state, the moisture flux and wind fields at 750 hPa indicate that an apparent anomalous circulation similar to an anticyclone (here we defined quasi-anticyclone) developed in the Arabian Sea ( $40^\circ\text{E}$ – $90^\circ\text{E}$ ,  $10^\circ\text{N}$ – $30^\circ\text{N}$ ) (Figures 2f and 4b, Figures S5c, S5f, and S6f in Supporting Information S1). It is worth noting that the moisture within the quasi-anticyclone (anticyclone) center is very low, which resulted in little precipitation in the center. But this strong and vast quasi-anticyclone diverts large amounts of oceanic moisture from the Bay of Bengal and Arabian Sea. The oceanic moisture along the outer edges of the quasi-anticyclone (anticyclone) is spun and transported to the southern slope of the Himalayas via the western and

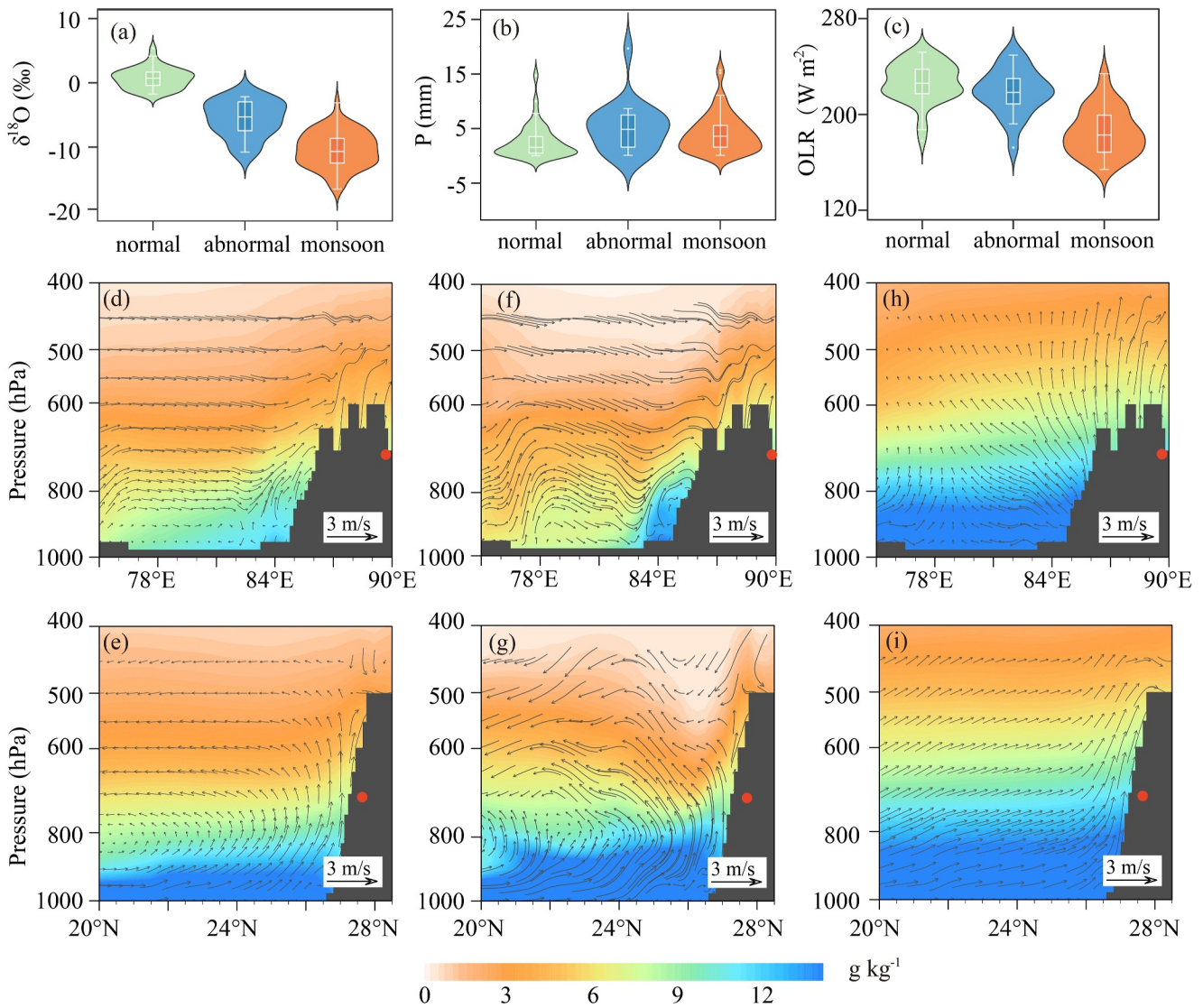


**Figure 3.** Violin plots showing the distribution of  $\delta^{18}\text{O}_p$  values (a), precipitation amount ( $P$ ) (b), and outgoing longwave radiation (c) during the pre-monsoon (the normal state and abnormal cases) and monsoon seasons in 2018. Cross sections of the zonal (d, f, h) and meridional (e, g, i) winds at vertical levels with total water contents (water vapor plus liquid and ice water content) during the pre-monsoon (d, e, f, g) and monsoon (h, i) seasons in 2018. Panels (d, e) represent the normal state during the pre-monsoon season. Panels (f, g) represent the abnormal cases during the pre-monsoon season in 2018 (7 May 2018 was selected as an example). The black shadows represent the terrain, the red dot represents the Asang station, colored shadows represent total water contents, and arrow represents the wind.

northern coasts of the Arabian Sea by this quasi-anticyclone. Compared with the normal state, the pathway of the moisture transported by the quasi-anticyclone is longer, and the rainout effect becomes stronger. This stronger rainout effect results in the abnormally low  $\delta^{18}\text{O}_p$  values at our study station. As shown in Figures 2d and 2e, we can find that similar patterns occur at the 600 and 500 hPa levels to 750 hPa (Figure 2f), although the moisture flux gradually decreases from 750 to 500 hPa.

In the vertical direction, the cross sections of zonal and meridional winds at vertical levels with total water contents also show that the moisture can be uplifted to higher altitudes (Figures 3f, 3g, and 4b, Figures S8f and S8g in Supporting Information S1). Usually, the higher altitudes correspond to lower air temperatures, which leads to greater condensation (Yu et al., 2016, 2017). As a result, the  $\delta^{18}\text{O}_p$  values at our study station become further depleted for the abnormal cases due to uplift processes during the pre-monsoon season (Figure 3a).

Similar abnormally low  $\delta^{18}\text{O}_p$  values occur at the nearby stations (Tezpur, Darjeeling, and Kathmandu) for the abnormal cases during the pre-monsoon season in different years (Figures S2e–S2g, S3e–S3g, and S4e–S4g in

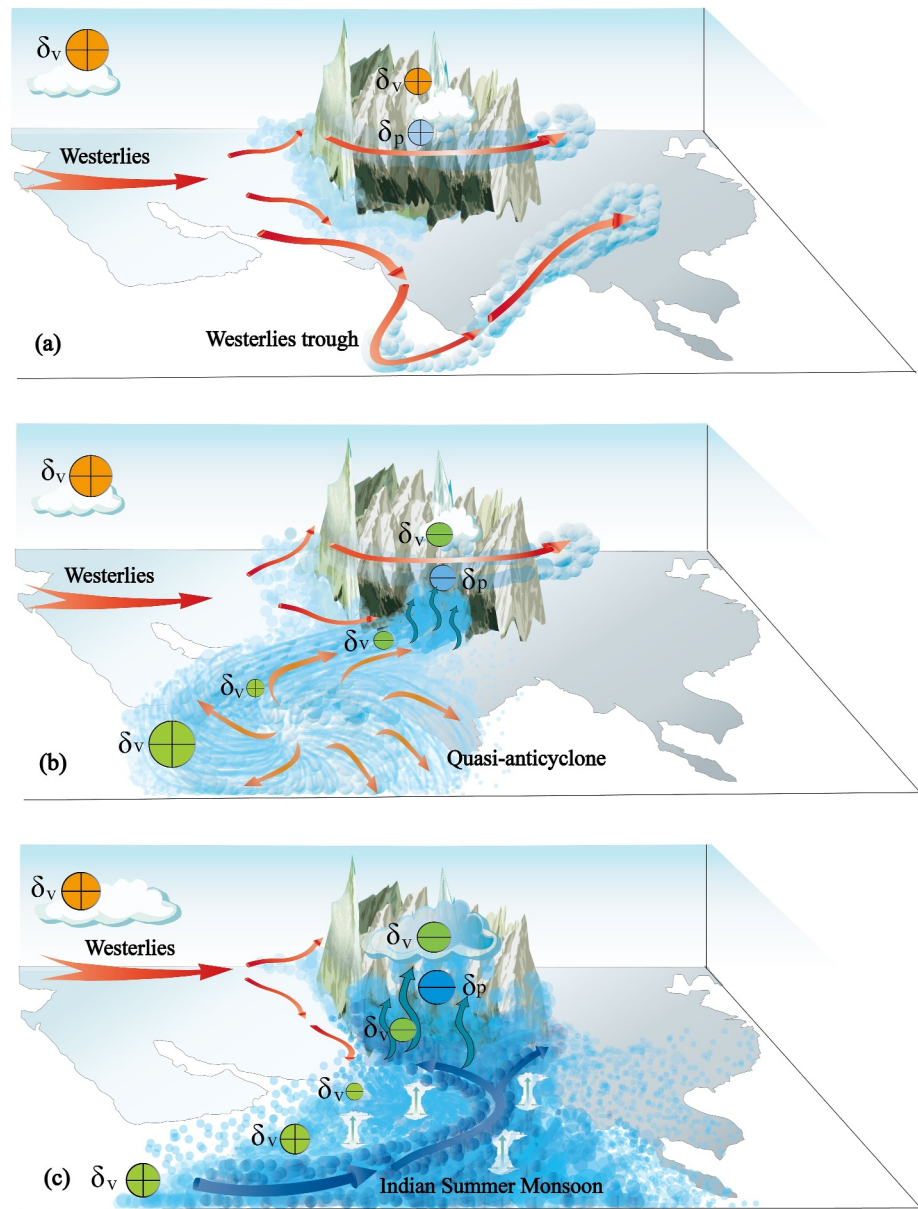


**Figure 4.** Schematic diagram of Indian Ocean moisture transported to the southern slope of central Himalayas over different seasons. (a) The normal state during the pre-monsoon season, (b) the abnormal cases (the quasi-anticyclone develops) during the pre-monsoon season, (c) the monsoon season. Moisture transport (arrows), moisture (blue bubble), vapor stable isotopes ( $\delta_v$ ) transported by the westerlies (orange circle) and Indian summer monsoon (green circle) all affect precipitation stable isotopes ( $\delta_p$ ) in the study region (blue circle). The water vapor isotopic data along the westerlies and Indian summer monsoon were retrieved from some studies (Angert et al., 2008; Rahul et al., 2016; Tang, 2009). Note the plus (minus) signs within the circles that indicate increased (decreased) values, and the sizes of the circles show the magnitudes of those increases (decreases).

Supporting Information S1) and are also attributed to these anomalous circulation events. It should be noted that the  $\delta^{18}\text{O}_p$  values from the Tezpur ( $-2.69\text{‰}$ ) and Kathmandu ( $-2.90\text{‰}$ ) stations are not as low as those from the Asang station for the abnormal cases during the pre-monsoon season. This is because both Tezpur (48 m a.s.l.) and Kathmandu (1,400 m a.s.l.) stations are located in basins, and the moisture cannot be uplifted to higher altitudes without the elevated terrain. However, the altitude of Darjeeling (2,042 m a.s.l.) is similar to Asang and so the  $\delta^{18}\text{O}_p$  values at Darjeeling ( $-12.55\text{‰}$ ) during the abnormal cases are comparable to Asang. This result

indicates that the uplift effect from the high altitude terrain plays an important role in moisture transport for the abnormal cases and the results from the nearby stations strengthen our conclusions.

It is worth noting that the location and size of the quasi-anticyclone changes over time, and the corresponding  $\delta^{18}\text{O}_p$  values also changes in response. For example, compared with 28 March in 2018 and 26 March in 2019 (Figures 2d–2f, Figures S6d–6f in Supporting Information S1), the centers of the quasi-anticyclone events on 6 April and 9 April in 2019 (Figure S7 in Supporting Information S1) move to the east and south, and the sizes of the quasi-anticyclone events become smaller. In this case, the ocean area “swept” by the quasi-anticyclone is smaller, the moisture transport pathways become shorter, and the rainout effect becomes weaker. Consequently, the  $\delta^{18}\text{O}_p$  values on 6 April ( $-2.32\text{‰}$ ) and 9 April ( $-3.70\text{‰}$ ) in 2019 were less decreased than on 28 March in 2018 ( $-5.21\text{‰}$ ) and 26 March in 2019 ( $-7.21\text{‰}$ ). More evidences come from the similar cases of 12 and 13 April 2018 (the figures are omitted). This result suggests that the quasi-anticyclone not only causes the abnormally low  $\delta^{18}\text{O}_p$  values, but its size and location also influence the magnitude of the  $\delta^{18}\text{O}_p$  values during this period.

In addition, on 8 and 9 February and 16 April in 2019, the quasi-anticyclone moved eastward to the Bay of Bengal, and became a strong anticyclone (Figure S9a in Supporting Information S1). Meanwhile, a westerlies trough developed at the northwestern part of the Indian subcontinent (Figure S9 in Supporting Information S1). Like two counter-rotating gears, the southwest wind formed at the front of the westerlies trough, and strengthened by the anticyclone, resulted in remote and abundant Indian Ocean moisture to be transported to the southern slope of central Himalayas (Figures S9, and S10 in Supporting Information S1). The westerlies trough combined with the anticyclone also caused the abnormally low  $\delta^{18}\text{O}_p$  values ( $-4.70\text{‰}$  and  $-6.89\text{‰}$  for 8 and 9 February 2019, respectively) and heavy precipitation (28.1 and 10.9 mm for 8 and 9 February in 2019, respectively). Hence, the anomalous circulations (the quasi-anticyclone, anticyclone, and/or westerlies trough) contributed to the abnormal precipitation and the abnormally low  $\delta^{18}\text{O}_p$  values on the southern slope of central Himalayas during the pre-monsoon season. Furthermore, the magnitude of the decrease in pre-monsoon  $\delta^{18}\text{O}_p$  values is dependent on the location and size of quasi-anticyclone.

#### 4.2. The Relationships Between $\delta^{18}\text{O}_p$ and the Indian Summer Monsoon Combined With Convection

During the monsoon season, the moisture flux and wind fields indicate that the Indian summer monsoon prevails over this period (Figures 2f, 2h, 2i, Figures S6f, S6h, and S6i in Supporting Information S1). As one of the most energetic components of the climate system (M. B. Allen & Armstrong, 2012; Gadgil, 2003; Webster et al., 1998), the Indian summer monsoon delivers a large amount of moisture from the remote southwest Indian Ocean over a wide moisture transport range ( $0^\circ\text{N}$ – $30^\circ\text{N}$  and  $60^\circ\text{E}$ – $110^\circ\text{E}$ ) including the southern slope of central Himalayas. It is clear that the moisture available in this region is more abundant than for other seasons (Figures 2f, 2h, 2i, Figures S6f, S6h, and S6i in Supporting Information S1). Compared with the abnormal cases during the pre-monsoon season, the Indian summer monsoon has much larger power to push the oceanic moisture northward and the abundant moisture can then be lifted by the Himalayas to higher altitudes (Figure 3i, Figures S4i, and S4c in Supporting Information S1). Hence, the stronger uplift effect causes lower  $\delta^{18}\text{O}_p$  values during the monsoon season in agreement with previous studies (Biggs et al., 2015; Gonfiantini et al., 2001; Gourcy et al., 2022; Holdsworth et al., 1991; Yu et al., 2017). Moreover, strong convection also occurs frequently over the Bay of Bengal and Indian subcontinent during this period (Figures 3c, 3h, and 4c, Figures S8c and S8h in Supporting Information S1) (Bhardwaj et al., 2019; Pattanaik, 2007). In this case, the moisture can be uplifted to higher altitudes where the air temperatures are lower, and the condensation becomes stronger. This process also contributes to the lower  $\delta^{18}\text{O}_p$  values during the monsoon season. Conclusively, the Indian summer monsoon combined with convection causes the lower  $\delta^{18}\text{O}_p$  values at Asang compared to the other seasons. Similarly, the Indian summer monsoon combined with convection also causes the lower  $\delta^{18}\text{O}_p$  values measured at the nearby stations including Tezpur, Darjeeling, and Kathmandu during the monsoon season (Figures S2h–S2j, S3h–S3j, and S4h–S4j in Supporting Information S1).

Conversely, occasional relatively high  $\delta^{18}\text{O}_p$  values with lower precipitation amounts are also recorded during the monsoon season. For example, the  $\delta^{18}\text{O}_p$  values on 8 August 2018 and 17 July 2019 were  $-3.11\text{‰}$  and  $-1.60\text{‰}$ , and the corresponding precipitation amounts were 2.4 and 3.4 mm, respectively. It is possible that lower precipitation amounts with smaller raindrops and slower falling speeds, results in stronger sub-cloud secondary evaporation (S. T. Allen et al., 2017; Managave et al., 2016; Salamalikis et al., 2016). This process may contribute to the relatively high  $\delta^{18}\text{O}_p$  for these cases during the monsoon season.



During the post-monsoon season, the Indian summer monsoon weakens and retreats and the westerlies strengthen and regain control of our study area. In this case, the precipitation amount reduces and the corresponding  $\delta^{18}\text{O}_p$  values become relatively high (Figure 1d).

## 5. Conclusion

This study investigated the seasonal patterns of  $\delta^{18}\text{O}_p$  values at the Asang station on the southern slope of central Himalayas and discussed the influence of the Indian Ocean moisture driven by the different dynamics on the  $\delta^{18}\text{O}_p$  over different seasons. Our findings show that, during the pre-monsoon season, for the normal state, moisture sourced from the Mediterranean region and the Atlantic Ocean and delivered by the westerlies produced relatively high  $\delta^{18}\text{O}_p$  values. Sub-cloud secondary evaporation also likely contributed the relatively high  $\delta^{18}\text{O}_p$  values. For the abnormal cases during the pre-monsoon season, under the influence of the development of a quasi-anticyclone, the moisture was driven from the Bay of Bengal and the Arabian Sea in turn, and then was spun northward to the southern slopes of central Himalayas via the western and northern coasts of the Arabian Sea. The relatively long moisture transport pathway caused strong rainout effects and led to the abnormally low  $\delta^{18}\text{O}_p$  values measured at the study site during the pre-monsoon season. Moreover, the magnitude of the abnormal decrease in  $\delta^{18}\text{O}_p$  values during the pre-monsoon season depended on the location and size of the quasi-anticyclone. Abnormally low  $\delta^{18}\text{O}_p$  values also occurred when the quasi-anticyclone became an anticyclone in combination with a westerlies trough. In comparison, during the monsoon season, the Indian summer monsoon combined with increased convection caused stronger rainout and uplift effects and resulted in the much lower and persistent  $\delta^{18}\text{O}_p$  values compared to other seasons.

Generally, the low/high stable isotopic values of ice cores and tree rings from central Himalayas are commonly used to reconstruct the strong/weak monsoon (Pang et al., 2014; Sano et al., 2013). However, we found that abnormally low  $\delta^{18}\text{O}_p$  values can also appear during the pre-monsoon season that corresponded to heavy precipitation. For ice core records, heavy snow deposited on the glaciers of central Himalayas during the pre-monsoon season is more difficult to melt than during the monsoon season. In contrast, during the monsoon season, glacial ice (or heavy snow deposited on the glaciers) is easier to melt. As observed by Liu et al. (2021) on the East Rongbuk glacier (the northern of the Everest), the ablation total was 425 mm water equivalent at 6,523 m a.s.l. during the period 10 June–22 July 2005. In this case, the isotopic signals of the heavy snow during the pre-monsoon season can form a more important part of the ice core record. Therefore, if the abnormally low  $\delta^{18}\text{O}_p$  values during the pre-monsoon season are not considered, the paleoclimate reconstruction using stable isotope records of ice cores would likely have increased uncertainty.

In addition, a robust understanding of these anomalous circulations during the pre-monsoon season is helpful to explore extreme rainfall or snowfall events, glacier changes and vegetation growth. Our study found that the abnormally low  $\delta^{18}\text{O}_p$  values are closely linked to the anomalous circulations during the pre-monsoon season. Hence, the abnormally low  $\delta^{18}\text{O}_p$  values during the pre-monsoon season can be used to track the anomalous circulation. Moreover,  $\delta^{18}\text{O}$  records preserved in ice core and tree ring archives from central Himalayas may have potential to act as indicators to reconstruct occurrences of anomalous circulation.

## Data Availability Statement

Sources of the data used in this study are as follows: The measured data are available at Yu and Lazhu (2023). The ERA5 reanalysis data on pressure levels including U-component of wind, V-component of wind, specific humidity, specific cloud ice water content, and specific cloud liquid water content are available at Hersbach et al. (2023a). The ERA5 reanalysis data on single levels including mean top net long-wave radiation flux are available at Hersbach et al. (2023b).

## References

- Acharya, S., Yang, X., Yao, T., & Shrestha, D. (2020). Stable isotopes of precipitation in Nepal Himalaya highlight the topographic influence on moisture transport. *Quaternary International*, 565, 22–30. <https://doi.org/10.1016/j.quaint.2020.09.052>
- Adhikari, N., Gao, J., Yao, T., Yang, Y., & Dai, D. (2020). The main controls of the precipitation stable isotopes at Kathmandu, Nepal. *Tellus B: Chemical and Physical Meteorology*, 72(1), 1–17. <https://doi.org/10.1080/16000889.2020.1721967>
- Allen, M. B., & Armstrong, H. A. (2012). Reconciling the Intertropical Convergence Zone, Himalayan/Tibetan tectonics, and the onset of the Asian monsoon system. *Journal of Asian Earth Sciences*, 44, 36–47. <https://doi.org/10.1016/j.jseas.2011.04.018>

## Acknowledgments

This study was supported by the Basic Science Center for Tibetan Plateau Earth System (BSCTPES, NSFC project no. 41988101-03) and the National Natural Science Foundation of China (42171122). Special thanks are given to the editor (Dr. Anantha Aiyyer) and two anonymous reviewers for their constructive comments.

- Allen, S. T., Keim, R. F., Barnard, H. R., McDonnell, J. J., & Renée Brooks, J. (2017). The role of stable isotopes in understanding rainfall interception processes: A review. *Wiley Interdisciplinary Reviews: Water*, 4(1), e1187. <https://doi.org/10.1002/wat2.1187>
- Angert, A., Lee, J. E., & Yakir, D. A. N. (2008). Seasonal variations in the isotopic composition of near-surface water vapour in the eastern Mediterranean. *Tellus B: Chemical and Physical Meteorology*, 60(4), 674–684. <https://doi.org/10.1111/j.1600-0889.2008.00357.x>
- Axelsson, J., Gao, J., Eckhardt, S., Cassiani, M., Chen, D., & Zhang, Q. (2023). A precipitation isotopic response in 2014–2015 to moisture transport changes in the central Himalayas. *Journal of Geophysical Research: Atmospheres*, 128(13), e2023JD038568. <https://doi.org/10.1029/2023JD038568>
- Bhardwaj, P., Pattanaik, D. R., & Singh, O. (2019). Tropical cyclone activity over Bay of Bengal in relation to El Niño-Southern Oscillation. *International Journal of Climatology*, 39(14), 5452–5469. <https://doi.org/10.1002/joc.6165>
- Biemans, H., Siderius, C., Lutz, A. F., Nepal, S., Ahmad, B., Hassan, T., et al. (2019). Importance of snow and glacier meltwater for agriculture on the Indo-Gangetic Plain. *Nature Sustainability*, 2(7), 594–601. <https://doi.org/10.1038/s41893-019-0305-3>
- Biggs, T. W., Lai, C. T., Chandan, P., Lee, R. M., Messina, A., Leshner, R. S., & Khatoun, N. (2015). Evaporative fractions and elevation effects on stable isotopes of high elevation lakes and streams in arid western Himalaya. *Journal of Hydrology*, 522, 239–249. <https://doi.org/10.1016/j.jhydrol.2014.12.023>
- Bolch, T., Kulkarni, A., Kääb, A., Huggel, C., Paul, F., Cogley, J. G., et al. (2012). The state and fate of Himalayan glaciers. *Science*, 336(6079), 310–314. <https://doi.org/10.1126/science.121518>
- Bookhagen, B., & Burbank, D. W. (2006). Topography, relief, and TRMM-derived rainfall variations along the Himalaya. *Geophysical Research Letters*, 33(8), L08405. <https://doi.org/10.1029/2006GL026037>
- Bookhagen, B., & Burbank, D. W. (2010). Toward a complete Himalayan hydrological budget: Spatiotemporal distribution of snowmelt and rainfall and their impact on river discharge. *Journal of Geophysical Research*, 115(F3), F03019. <https://doi.org/10.1029/2009JF001426>
- Bowen, G. J., & Wilkinson, B. (2002). Spatial distribution of  $\delta^{18}\text{O}$  in meteoric precipitation. *Geology*, 30(4), 315–318. [https://doi.org/10.1130/0091-7613\(2002\)030<0315:SDOIM>2.0.CO;2](https://doi.org/10.1130/0091-7613(2002)030<0315:SDOIM>2.0.CO;2)
- Brunello, C. F., Andermann, C., Helle, G., Comiti, F., Tonon, G., Tiwari, A., & Hovius, N. (2019). Hydroclimatic seasonality recorded by tree ring  $\delta^{18}\text{O}$  signature across a Himalayan altitudinal transect. *Earth and Planetary Science Letters*, 518, 148–159. <https://doi.org/10.1016/j.epsl.2019.04.030>
- Chakraborty, S., Burman, P. K. D., Sarma, D., Sinha, N., Datye, A., Metya, A., et al. (2022). Linkage between precipitation isotopes and biosphere-atmosphere interaction observed in northeast India. *npj Climate and Atmospheric Science*, 5(1), 10. <https://doi.org/10.1038/s41612-022-00231-z>
- Chakraborty, S., Sinha, N., Chattopadhyay, R., Sengupta, S., Mohan, P. M., & Datye, A. (2016). Atmospheric controls on the precipitation isotopes over the Andaman Islands, Bay of Bengal. *Scientific Reports*, 6(1), 19555. <https://doi.org/10.1038/srep19555>
- Curio, J., Maussion, F., & Scherer, D. (2015). A 12-year high-resolution climatology of atmospheric water transport over the Tibetan Plateau. *Earth System Dynamics*, 6(1), 109–124. <https://doi.org/10.5194/esd-6-109-2015>
- Fasullo, J., & Webster, P. J. (2003). A hydrological definition of Indian monsoon onset and withdrawal. *Journal of Climate*, 16(19), 3200–3211. [https://doi.org/10.1175/1520-0442\(2003\)016<3200a:AHDOIM>2.0.CO;2](https://doi.org/10.1175/1520-0442(2003)016<3200a:AHDOIM>2.0.CO;2)
- Feng, L., & Zhou, T. (2012). Water vapor transport for summer precipitation over the Tibetan Plateau: Multidata set analysis. *Journal of Geophysical Research*, 117(D20), D200114. <https://doi.org/10.1029/2011JD017012>
- Gadgil, S. (2003). The Indian monsoon and its variability. *Annual Review of Earth and Planetary Sciences*, 31(1), 429–467. <https://doi.org/10.1146/annurev.earth.31.100901.141251>
- Gao, J. (2020). Hydrogen and oxygen stable isotope data set of Kathmandu precipitation (2016–2018). *National Tibetan Plateau/Third Pole Environment Data Center*. <https://doi.org/10.11888/Meteoro.tpcd.270936>
- Gao, J., Masson-Delmotte, V., Yao, T., Tian, L., Risi, C., & Hoffmann, G. (2011). Precipitation water stable isotopes in the south Tibetan Plateau: Observations and modeling. *Journal of Climate*, 24(13), 3161–3178. <https://doi.org/10.1175/2010JCLI3736.1>
- Gonfiantini, R., Roche, M. A., Olivry, J. C., Fontes, J. C., & Zuppi, G. M. (2001). The altitude effect on the isotopic composition of tropical rains. *Chemical Geology*, 181(1–4), 147–167. [https://doi.org/10.1016/S0009-2541\(01\)00279-0](https://doi.org/10.1016/S0009-2541(01)00279-0)
- Gourcy, L., Adamson, J. K., Miner, W. J., Vitvar, T., & Belizaire, D. (2022). The use of water stable isotopes for a better understanding of hydrogeological processes in Haiti: Overview of existing  $\delta^{18}\text{O}$  and  $\delta^2\text{H}$  data. *Hydrogeology Journal*, 30(5), 1387–1397. <https://doi.org/10.1007/s10040-022-02498-1>
- Hersbach, H., Bell, B., Berrisford, P., Biavati, G., Horányi, A., Muñoz Sabater, J., et al. (2023a). ERA5 hourly data on pressure levels from 1940 to present [Dataset]. *Copernicus Climate Change Service (C3S) Climate Data Store (CDS)*. <https://doi.org/10.24381/cds.bd0915c6>
- Hersbach, H., Bell, B., Berrisford, P., Biavati, G., Horányi, A., Muñoz Sabater, J., et al. (2023b). ERA5 hourly data on single levels from 1940 to present [Dataset]. *Copernicus Climate Change Service (C3S) Climate Data Store (CDS)*. <https://doi.org/10.24381/cds.adbb2d47>
- Holdsworth, G., Fogarasi, S., & Krouse, H. R. (1991). Variation of the stable isotopes of water with altitude in the Saint Elias Mountains of Canada. *Journal of Geophysical Research*, 96(D4), 7483–7494. <https://doi.org/10.1029/91JD00048>
- Hou, S., Zhang, W., Pang, H., Wu, S. Y., Jenk, T. M., Schwikowski, M., & Wang, Y. (2019). Apparent discrepancy of Tibetan ice core  $\delta^{18}\text{O}$  records may be attributed to misinterpretation of chronology. *The Cryosphere*, 13(6), 1743–1752. <https://doi.org/10.5194/tc-13-1743-2019>
- Hren, M. T., Bookhagen, B., Blisniuk, P. M., Booth, A. L., & Chamberlain, C. P. (2009).  $\delta^{18}\text{O}$  and  $\delta\text{D}$  of streamwaters across the Himalaya and Tibetan Plateau: Implications for moisture sources and paleoelevation reconstructions. *Earth and Planetary Science Letters*, 288(1–2), 20–32. <https://doi.org/10.1016/j.epsl.2009.08.041>
- Hussain, S., Xianfang, S., Hussain, I., Jianrong, L., Dong Mei, H., Li Hu, Y., & Huang, W. (2015). Controlling factors of the stable isotope composition in the precipitation of Islamabad, Pakistan. *Advances in Meteorology*, 2015, 1–11. <https://doi.org/10.1155/2015/817513>
- Immerzeel, W. W., Van Beek, L. P., & Bierkens, M. F. (2010). Climate change will affect the Asian water towers. *Science*, 328(5984), 1382–1385. <https://doi.org/10.1126/science.1183188>
- Islam, M. R., Gao, J., Ahmed, N., Karim, M. M., Bhuiyan, A. Q., Ahsan, A., & Ahmed, S. (2021). Controls on spatiotemporal variations of stable isotopes in precipitation across Bangladesh. *Atmospheric Research*, 247, 105224. <https://doi.org/10.1016/j.atmosres.2020.105224>
- Jeelani, G., & Deshpande, R. D. (2017). Isotope fingerprinting of precipitation associated with western disturbances and Indian summer monsoons across the Himalayas. *Journal of Earth System Science*, 126(8), 1–13. <https://doi.org/10.1007/s12040-017-0894-z>
- Jeelani, G., Deshpande, R. D., Galkowski, M., & Rozanski, K. (2018). Isotopic composition of daily precipitation along the southern foothills of the Himalayas: Impact of marine and continental sources of atmospheric moisture. *Atmospheric Chemistry and Physics*, 18(12), 8789–8805. <https://doi.org/10.5194/acp-18-8789-2018>
- Jing, Z., Yu, W., Lewis, S., Thompson, L. G., Xu, J., Zhang, J., et al. (2022). Inverse altitude effect disputes the theoretical foundation of stable isotope paleoaltimetry. *Nature Communications*, 13(1), 4371. <https://doi.org/10.1038/s41467-022-32172-9>

- Kang, S., Mayewski, P. A., Qin, D., Yan, Y., Hou, S., Zhang, D., et al. (2002). Glaciochemical records from a Mt. Everest ice core: Relationship to atmospheric circulation over Asia. *Atmospheric Environment*, 36(21), 3351–3361. [https://doi.org/10.1016/S1352-2310\(02\)00325-4](https://doi.org/10.1016/S1352-2310(02)00325-4)
- Konecky, B. L., Noone, D. C., & Cobb, K. M. (2019). The influence of competing hydroclimate processes on stable isotope ratios in tropical rainfall. *Geophysical Research Letters*, 46(3), 1622–1633. <https://doi.org/10.1029/2018GL080188>
- Lang, T. J., & Barros, A. P. (2004). Winter storms in the central Himalayas. *Journal of the Meteorological Society of Japanese Series II*, 82(3), 829–844. <https://doi.org/10.2151/jmsj.2004.829>
- Liu, W., Zhang, D., Qin, X., van den Broeke, M. R., Jiang, Y., Yang, D., & Ding, M. (2021). Monsoon clouds control the summer surface energy balance on East Rongbuk glacier (6,523 m above sea level), the northern of Mt. Qomolangma (Everest). *Journal of Geophysical Research: Atmospheres*, 126(8), e2020JD033998. <https://doi.org/10.1029/2020JD033998>
- Madhura, R. K., Krishnan, R., Revadekar, J. V., Mujumdar, M., & Goswami, B. N. (2015). Changes in western disturbances over the Western Himalayas in a warming environment. *Climate Dynamics*, 44(3–4), 1157–1168. <https://doi.org/10.1007/s00382-014-2166-9>
- Managave, S. R., Jani, R. A., Narayana Rao, T., Sunilkumar, K., Satheeshkumar, S., & Ramesh, R. (2016). Intra-event isotope and raindrop size data of tropical rain reveal effects concealed by event averaged data. *Climate Dynamics*, 47(3–4), 981–987. <https://doi.org/10.1007/s00382-015-2884-7>
- Pan, C., Zhu, B., Gao, J., Kang, H., & Zhu, T. (2019). Quantitative identification of moisture sources over the Tibetan Plateau and the relationship between thermal forcing and moisture transport. *Climate Dynamics*, 52(1–2), 181–196. <https://doi.org/10.1007/s00382-018-4130-6>
- Pang, H., Hou, S., Kaspari, S., & Mayewski, P. A. (2014). Influence of regional precipitation patterns on stable isotopes in ice cores from the central Himalayas. *The Cryosphere*, 8(1), 289–301. <https://doi.org/10.5194/tc-8-289-2014>
- Pattanaik, D. R. (2007). Variability of convective activity over the North Indian Ocean and its associations with monsoon rainfall over India. *Pure and Applied Geophysics*, 164(8–9), 1527–1545. <https://doi.org/10.1007/s00024-007-0243-2>
- Rahul, P., & Ghosh, P. (2019). Long term observations on stable isotope ratios in rainwater samples from twin stations over Southern India; identifying the role of amount effect, moisture source and rainout during the dual monsoons. *Climate dynamics*, 52(11), 6893–6907. <https://doi.org/10.1007/s00382-018-4552-1>
- Rahul, P., Ghosh, P., Bhattacharya, S. K., & Yoshimura, K. (2016). Controlling factors of rainwater and water vapor isotopes at Bangalore, India: Constraints from observations in 2013 Indian monsoon. *Journal of Geophysical Research: Atmospheres*, 121(23), 13936–13952. <https://doi.org/10.1002/2016JD025352>
- Ren, W., Yao, T., & Xie, S. (2017). Key drivers controlling the stable isotopes in precipitation on the leeward side of the central Himalayas. *Atmospheric research*, 189, 134–140. <https://doi.org/10.1016/j.atmosres.2017.01.020>
- Salamalikis, V., Argiriou, A. A., & Dotsika, E. (2016). Isotopic modeling of the sub-cloud evaporation effect in precipitation. *Science of the Total Environment*, 544, 1059–1072. <https://doi.org/10.1016/j.scitotenv.2015.11.072>
- Sano, M., Tshering, P., Komori, J., Fujita, K., Xu, C., & Nakatsuka, T. (2013). May–September precipitation in the Bhutan Himalaya since 1743 as reconstructed from tree ring cellulose  $\delta^{18}\text{O}$ . *Journal of Geophysical Research: Atmospheres*, 118(15), 8399–8410. <https://doi.org/10.1002/jgrd.50664>
- Scherler, D., Bookhagen, B., & Strecker, M. R. (2011). Spatially variable response of Himalayan glaciers to climate change affected by debris cover. *Nature Geoscience*, 4(3), 156–159. <https://doi.org/10.1038/ngeo1068>
- Sharma, S. S., & Ganju, A. (2000). Complexities of avalanche forecasting in Western Himalaya—An overview. *Cold Regions Science and Technology*, 31(2), 95–102. [https://doi.org/10.1016/S0165-232X\(99\)00034-8](https://doi.org/10.1016/S0165-232X(99)00034-8)
- Shrestha, A. B., & Aryal, R. (2011). Climate change in Nepal and its impact on Himalayan glaciers. *Regional Environmental Change*, 11(S1), 65–77. <https://doi.org/10.1007/s10113-010-0174-9>
- Singh, N., Shekhar, M., Parida, B. R., Gupta, A. K., Sain, K., Rai, S. K., et al. (2022). Tree-ring isotopic records suggest seasonal importance of moisture dynamics over glacial valleys of the central Himalaya. *Frontiers in Earth Science*, 10, 868357. <https://doi.org/10.3389/feart.2022.868357>
- Singh, N., Shekhar, M., Singh, J., Gupta, A. K., Bräuning, A., Mayr, C., & Singhal, M. (2021). Central Himalayan tree-ring isotopes reveal increasing regional heterogeneity and enhancement in ice mass loss since the 1960s. *The Cryosphere*, 15(1), 95–112. <https://doi.org/10.5194/tc-15-95-2021>
- Sinha, N., Chakraborty, S., Chattopadhyay, R., Goswami, B. N., Mohan, P., Parua, D. K., et al. (2019). Isotopic investigation of the moisture transport processes over the Bay of Bengal. *Journal of Hydrology X*, 2, 100021. <https://doi.org/10.1016/j.hydro.2019.100021>
- Su, B., Xia, C., Chen, D., Ying, X., Huang, Y., Guo, R., et al. (2022). Mismatch between the population and meltwater changes creates opportunities and risks for global glacier-fed basins. *Science Bulletin*, 67(1), 9–12. <https://doi.org/10.1016/j.scib.2021.07.027>
- Tang, W. (2009). *Atmospheric vapor isotope and the moisture transport in Southern Tibetan Plateau (in Chinese)*. (Doctoral dissertation). Institute of Tibetan Plateau Research, Chinese Academy of Sciences, National Science Library, Chinese Academy of Sciences, Beijing, China. Retrieved from <http://dpaper.las.ac.cn/Dpaper/homeNew>
- Thompson, L. G., Yao, T., Mosley-Thompson, E., Davis, M. E., Henderson, K. A., & Lin, P.-N. (2000). A high-resolution millennial record of the South Asian Monsoon from Himalayan ice cores. *Science*, 289(5486), 1916–1920. <https://doi.org/10.1126/science.289.5486.1916>
- Tian, L., Yao, T., White, J. W. C., Yu, W., & Wang, N. (2005). Westerly moisture transport to the middle of Himalayas revealed from the high deuterium excess. *Chinese Science Bulletin*, 50(10), 1026–1030. <https://doi.org/10.1360/04wd0030>
- Wang, S. Y. S., Gillies, R. R., Fosu, B., & Singh, P. M. (2015). The deadly Himalayan snowstorm of October 2014: Synoptic conditions and associated trends. *Bulletin of the American Meteorological Society*, 96(12), S89–S94. <https://doi.org/10.1175/bams-d-15-00113.1>
- Webster, P. J., Magana, V. O., Palmer, T. N., Shukla, J., Tomas, R. A., Yanai, M. U., & Yasunari, T. (1998). Monsoons: Processes, predictability, and the prospects for prediction. *Journal of Geophysical Research*, 103(C7), 14451–14510. <https://doi.org/10.1029/97JC02719>
- Yao, T., Masson-Delmotte, V., Gao, J., Yu, W., Yang, X., Risi, C., et al. (2013). A review of climatic controls on  $\delta^{18}\text{O}$  in precipitation over the Tibetan Plateau: Observations and simulations. *Reviews of Geophysics*, 51(4), 525–548. <https://doi.org/10.1002/rog.20023>
- Yao, T., Thompson, L. G., Shi, Y., Qin, D., Jiao, K., Yang, Z., et al. (1997). Climate variation since the last interglaciation recorded in the Guliya ice core. *Science in China Series D: Earth Sciences*, 40(6), 662–668. <https://doi.org/10.1007/BF02877697>
- Yu, W., & Lazhu. (2023). Measured data at the Asang station on the southern slope of the central Himalayas during 2018–2019 [Dataset]. [figshare. https://doi.org/10.6084/m9.figshare.24657444.v4](https://doi.org/10.6084/m9.figshare.24657444.v4)
- Yu, W., Tian, L., Yao, T., Xu, B., Wei, F., Ma, Y., et al. (2017). Precipitation stable isotope records from the northern Hengduan Mountains in China capture signals of the winter India–Burma Trough and the Indian Summer Monsoon. *Earth and Planetary Science Letters*, 477, 123–133. <https://doi.org/10.1016/j.epsl.2017.08.018>
- Yu, W., Yao, T., Thompson, L. G., Jouzel, J., Zhao, H., Xu, B., et al. (2021). Temperature signals of ice core and speleothem isotopic records from Asian monsoon region as indicated by precipitation  $\delta^{18}\text{O}$ . *Earth and Planetary Science Letters*, 554, 116665. <https://doi.org/10.1016/j.epsl.2020.116665>

- Yu, W., Yao, T., Tian, L., Ma, Y., Wen, R., Devkota, L. P., et al. (2016). Short-term variability in the dates of the Indian monsoon onset and retreat on the southern and northern slopes of the central Himalayas as determined by precipitation stable isotopes. *Climate Dynamics*, *47*(1–2), 159–172. <https://doi.org/10.1007/s00382-015-2829-1>
- Zhang, G., Bolch, T., Yao, T., Rounce, D. R., Chen, W., Veh, G., et al. (2023). Underestimated mass loss from lake-terminating glaciers in the greater Himalaya. *Nature Geoscience*, *16*(4), 333–338. <https://doi.org/10.1038/s41561-023-01150-1>
- Zhang, J., Yu, W., Jing, Z., Lewis, S., Xu, B., Ma, Y., et al. (2021). Coupled effects of moisture transport pathway and convection on stable isotopes in precipitation across the East Asian monsoon region: Implications for paleoclimate reconstruction. *Journal of Climate*, *34*(24), 9811–9822. <https://doi.org/10.1175/JCLI-D-21-0271.1>

### References From the Supporting Information

- Qu, D., Tian, L., Zhao, H., Yao, P., Xu, B., & Cui, J. (2020). Demonstration of a memory calibration method in water isotope measurement by laser spectroscopy. *Rapid Communications in Mass Spectrometry*, *34*(8), e8689. <https://doi.org/10.1002/rcm.8689>
- Wang, X., Pang, G., & Yang, M. (2018). Precipitation over the Tibetan Plateau during recent decades: A review based on observations and simulations. *International Journal of Climatology*, *38*(3), 1116–1131. <https://doi.org/10.1002/joc.5246>
- Wassenaar, L., Terzer-Wassmuth, S., & Douence, C. (2021). Progress and challenges in dual-and triple-isotope ( $\delta^{18}\text{O}$ ,  $\delta^2\text{H}$ ,  $\Delta^{17}\text{O}$ ) analyses of environmental waters: An international assessment of laboratory performance. *Rapid Communications in Mass Spectrometry*, *35*(24), e9193. <https://doi.org/10.1002/rcm.9193>